

Dalton Transactions

Accepted Manuscript



This is an *Accepted Manuscript*, which has been through the Royal Society of Chemistry peer review process and has been accepted for publication.

Accepted Manuscripts are published online shortly after acceptance, before technical editing, formatting and proof reading. Using this free service, authors can make their results available to the community, in citable form, before we publish the edited article. We will replace this *Accepted Manuscript* with the edited and formatted *Advance Article* as soon as it is available.

You can find more information about *Accepted Manuscripts* in the [Information for Authors](#).

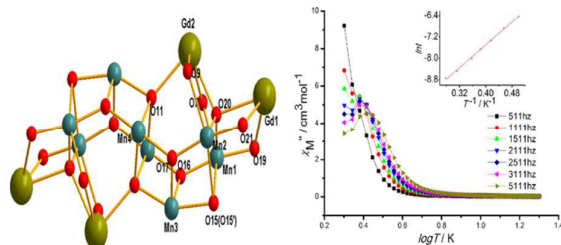
Please note that technical editing may introduce minor changes to the text and/or graphics, which may alter content. The journal's standard [Terms & Conditions](#) and the [Ethical guidelines](#) still apply. In no event shall the Royal Society of Chemistry be held responsible for any errors or omissions in this *Accepted Manuscript* or any consequences arising from the use of any information it contains.



www.rsc.org/dalton

Graphical Abstract

Dodendulcear Mn/Ln clusters with the 2-(hydroxymethyl)pyridine as ligand have been synthesized. Complexes **1** and **5** showed a frequency-dependent decrease in $\chi_M''T$ and out-of-phase χ_M'' peak maximum, indicating slow magnetic relaxation and potential SMM behaviour.



Cite this: DOI: 10.1039/c0xx00000x

www.rsc.org/xxxxxx

ARTICLE TYPE

Dodenuclear $[\text{Mn}^{\text{III}}_8\text{Ln}^{\text{III}}_4]$ Clusters with the 2-(hydroxymethyl)pyridine : Syntheses, Structures, and Magnetic Properties

Lei Sun^{a,b}, Hui Chen^a, Chengbing Ma^a and Changneng Chen^{a*}

Received (in XXX, XXX) Xth XXXXXXXXX 20XX, Accepted Xth XXXXXXXXX 20XX

DOI: 10.1039/b000000x

A new family of isostructural Mn/Ln dodenuclear clusters: $[\text{Mn}_8\text{Ln}_4(\text{O})_8(\text{hmp})_4(\text{O}_2\text{CPh})_{12}(\text{NO}_3)_4(\text{PhCO}_2\text{H})(\text{C}_2\text{H}_5\text{OH})]$ [Ln = La (1), Pr (2), Nd (3), Gd (4), Dy(5), hmpH = 2-(hydroxymethyl)pyridine] have been synthesized by the reaction of $\text{Mn}(\text{NO}_3)_2$ and $\text{Ln}(\text{NO}_3)_3 \cdot 6\text{H}_2\text{O}$ with hmpH and benzoic acid as co-ligands. Compounds 1–5 possess a spindle-shaped core of $[\text{Mn}^{\text{III}}_8\text{Ln}^{\text{III}}_4(\mu_4\text{-O})_4(\mu_3\text{-O})_4(\mu_3\text{-OR})_2(\mu_2\text{-OR})_8]^{10+}$, which composed of six face-sharing defected cubane units and two square-pyramidal units. The compounds represent the highest nuclearity Mn/Ln clusters with the use of hmpH to date. That the ferromagnetic interactions dominated within complexes 1–4 were suggested by solid-state dc magnetic susceptibility analyses. Compound 4 displays a magnetic-caloric effect (MCE) with $13.94 \text{ J Kg}^{-1} \text{ K}^{-1}$ of the entropy change at 6 K for $\Delta H = 8 \text{ T}$. Compounds 1 and 5 exhibit out-of-phase χ''_{m} peak maximum above 2.0 K. Fitting of the ac susceptibility data to an Arrhenius law give energy barrier $U_{\text{eff}} = 6.88/7.44 \text{ K}$ for compound 1 and 5 respectively.

Introduction

Single molecule magnets (SMMs) are individual molecules whose magnetic properties arise from a high energy barrier to reversal of the magnetisation leading to slow magnetization relaxation below a certain blocking temperature.¹ The upper limit to the energy barrier for SMMs should be summarized as $S^2|D|$ or $(S^2 - 1/4)|D|$ for integer and half-integer spins respectively, so the behaviour of SMMs is closely related to the combination of a large ground spin state (S) and a large zero field splitting parameters (D).² The exotic physical properties displayed by these complexes often include quantum tunneling of the magnetization, spin parity effects, and quantum phase interference.³ In last decade, polynuclear 3d–4f clusters have continuously drawn intense attention, for their versatile magnetic properties which have potential applications in the information storage.⁴ It is useful to investigate mixed 3d–4f complexes as SMMs, since mixing the transition metal and lanthanide ions in different proportions may modulate magnetic properties of such compounds. Since the first 3d–4f SMM of Cu_2Tb_2 ⁵ was discovered in 2004, various transition metals were successively applied to construct SMMs of this type,⁶ especially 3d metal manganese, which often displays high spin states and large zero field splitting parameters related to Jahn-Teller of Mn^{III} , such as Mn_2Ln_2 ,⁷ Mn_3Ln_4 ,⁸ Mn_4Ln_2 ,⁹ Mn_3Ln_4 ,^{10a} Mn_{12}Gd ,^{10b} and Mn_{18}Dy ^{10c} have been prepared. Nevertheless, the reports on mixed Mn/Ln complexes have been limited when compared with all Mn or all Ln compounds. Therefore, more Mn/Ln clusters need to be explored for searching other synthetic methods and further investigating the magnetic interactions.

On the other hand, magnetic cooler materials based on the magnetic-caloric effect (MCE) have emerged as attractive

candidates to replace the rare and expensive ³He in some ultralow temperature region.¹¹ MCE is associated with the change of magnetic entropy upon variation of the magnetic field, which could be applied to cooling technique via adiabatic demagnetization.¹² A large spin ground state and negligible anisotropy are essential for an ideal molecule refrigerant.¹³ The isotropic Gd^{III} (f^7) ion could be an ideal spin center candidate for magnetic cooler materials since it has a maximum entropy value calculated as $110 \text{ J Kg}^{-1} \text{ K}^{-1}$.^{13c} With this in mind, it will be worth for us investigating the MCE in mixed 3d-Gd complexes.

We oriented our research to construct a new family of polynuclear Mn/Ln clusters using pyridine-based alkoxide and small flexible carboxylate as co-ligands. The carboxylates ions are flexible ligands and widely used, which always lead to antiferromagnetic coupling. In order to enhance the ground state value of the clusters, we use the 2-(hydroxymethyl)pyridine (hmpH) to replace some of the carboxylates for its alkoxide O atom often supports ferromagnetic coupling between the metal atoms.¹⁴ The hmpH acts as a N/O bidentate chelate and bridging ligand and has proven to be an excellent ligand in the synthesis of high-nuclearity Mn species in the past (such as Mn_{10} ,¹⁵ Mn_{21} ,¹⁶ Mn_{12} ,¹⁷ Mn_{18} ¹⁸). However, to the best of our knowledge, hmpH has been employed in mixed Mn/Ln clusters with only three compounds: $\text{Mn}^{\text{III}}_2\text{Ln}^{\text{III}}_2$,^{19a} $\text{Mn}^{\text{III}}_2\text{Ln}^{\text{III}}_4$ ^{19b} and $\text{Mn}^{\text{III}}_4\text{Ce}^{\text{III}}_2$ ^{19c} reported to date. We herein reported the construction of a family of $\text{Mn}^{\text{III}}_8\text{Ln}^{\text{III}}_4$ clusters which possess the highest nuclearity in mixed Mn/Ln clusters based on hmp[−] as far as we are aware. Reactions of $\text{Mn}(\text{NO}_3)_2$ and $\text{Ln}(\text{NO}_3)_3 \cdot 6\text{H}_2\text{O}$ with hmpH and benzoic acid as co-ligands led to new examples of 3d/4f dodenuclear clusters. Magnetic susceptibility studies indicate the presence of ferromagnetic interactions within compounds 1–4

Cite this: DOI: 10.1039/c0xx00000x

www.rsc.org/xxxxxx

ARTICLE TYPE

Table 1 Crystallographic data for complexes 1–5

	1-0.5hmpH C ₁₂₀ H _{99.5} O _{51.5} N _{8.5} La ₄ Mn ₈	2-0.5hmpH C ₁₂₀ H _{99.5} O _{51.5} N _{8.5} Pr ₄ Mn ₈	3-0.5hmpH C ₁₂₀ H _{99.5} O _{51.5} N _{8.5} Nd ₄ Mn ₈	4-hmpH C ₁₂₃ H ₁₀₃ O ₅₂ N ₉ Gd ₄ Mn ₈	5-hmpH C ₁₂₃ H ₁₀₃ O ₅₂ N ₉ Dy ₄ Mn ₈
Formula					
Fw, g mol ⁻¹	3479	3487	3501	3607	3628
Crystal system	Triclinic	Triclinic	Triclinic	Triclinic	Triclinic
Space group	<i>P</i> -1	<i>P</i> -1	<i>P</i> -1	<i>P</i> -1	<i>P</i> -1
<i>a</i> , Å	14.3016(4)	14.3358(4)	14.3442(4)	14.3312(6)	14.3363(5)
<i>b</i> , Å	14.6971(3)	14.6448(2)	14.6164(3)	14.5625(4)	14.5705(5)
<i>c</i> , Å	17.1194(5)	17.0596(4)	17.0451(5)	17.0155(5)	17.0212(6)
<i>α</i> , deg	66.260(2)	66.305(2)	66.291(3)	66.290(3)	66.132(3)
<i>β</i> , deg	88.799(2)	88.319(2)	88.213(2)	88.429(3)	88.435(3)
<i>γ</i> , deg	84.005(2)	84.0997(1)	84.183(2)	84.120(3)	84.285(3)
<i>V</i> , Å ³	3274.99(15)	3261.98(13)	3255.03(15)	3233.88(19)	3234.95(18)
<i>Z</i>	1	1	1	1	1
<i>T</i> , K	100 K	100 K	100 K	100 K	100 K
ρ_{calcd} , g cm ⁻³	1.774	1.734	1.755	1.835	1.846
μ , mm ⁻¹	2.109	2.297	2.40	19.946	19.037
<i>F</i> (000)	1726	1691	1695	1711	1719
<i>R</i> ₁ ^a	0.050	0.0447	0.0433	0.0433	0.0455
<i>wR</i> ₂ ^c	0.1473	0.1174	0.1035	0.1084	0.1187

$$^a R_1 = \sum (|F_o| - |F_c|) / \sum |F_o|, \quad ^c wR_2 = [\sum w(F_o^2 - F_c^2)^2 / \sum w(F_o^2)^2]^{0.5}$$

and slow magnetization relaxation for compounds **1** and **5**. The Syntheses, structures, and magnetic properties of these compounds are described in this paper.

5 Experimental

Syntheses

All syntheses were performed under aerobic conditions. All reagents were commercially available and used without further purification.

10 Preparation of compounds **1–5**: Mn(NO₃)₂ (aq, 50%, 0.36ml, 1.5 mmol) and Ln(NO₃)₃·6H₂O (1.0 mmol) were added to a colorless stirred solution of hmpH (0.10 ml, 1.0 mmol) and NEt₃ (0.14 ml, 1.0 mmol) in MeCN (20 ml) and EtOH (5 ml), which led to a rapid color change to dark red. The solution was stirred for another 1 h
 15 at room temperature, solid benzoic acid (0.12 g, 1.0 mmol) was added under vigorous stirring. The mixture was stirred for further 4 h, then filtered, and the solution was left undisturbed in a flask. Slow evaporation of the solution at room temperature gave large black crystals in one week, which were collected by filtration,
 20 washed thoroughly with MeCN, and dried in vacuum.

[Mn₈La₄(O)₈(hmp)₄(O₂CPh)₁₂(NO₃)₄(PhCO₂H)(C₂H₅OH)] (1)
 Yield: 0.125 g, 19%. Elemental analysis (%) calcd for 1: C, 40.46; N, 3.60; H, 3.01. Found: C, 40.42; N, 3.73; H, 2.98. ICP analysis calcd for La: 15.73%. Found: 16.42%. Selected IR data
 25 (KBr, cm⁻¹): 3443 (mb), 3068 (w), 2843 (w), 1611 (s), 1577 (s), 1523 (m), 1482 (m), 1420 (s), 1380 (s), 1325 (m), 1257 (w), 1230 (w), 1169 (w), 1060 (m), 1018 (m), 855 (w), 814 (w), 774 (w), 719 (s), 678 (s), 623 (m), 603 (m), 562 (m), 467 (w), 427 (w).

[Mn₈Pr₄(O)₈(hmp)₄(O₂CPh)₁₂(NO₃)₄(PhCO₂H)(C₂H₅OH)] (2)
 30 Yield: 0.102 g, 16%. Elemental analysis (%) calcd for 2: C, 40.49; N, 3.79; H, 2.99. Found: C, 40.43; N, 3.78; H, 2.97. ICP analysis calcd for Pr: 15.93%. Found: 15.87%. Selected IR data
 (KBr, cm⁻¹): 3443 (mb), 2830 (w), 2367 (w), 1625 (s), 1570 (s),

1489 (m), 1468 (m), 1400 (s), 1304 (s), 1230 (m), 1188 (m),
 35 1155 (m), 1053 (s), 1032 (m), 856 (w), 821 (w), 760 (w), 719 (s), 672 (m), 637 (m), 589 (m), 556 (m), 467 (w), 427 (w).

[Mn₈Nd₄(O)₈(hmp)₄(O₂CPh)₁₂(NO₃)₄(PhCO₂H)(C₂H₅OH)] (3)

Yield: 0.098 g, 15%. Elemental analysis (%) calcd for 3: C, 40.36; N, 3.46; H, 2.89. Found: C, 40.32; N, 3.48; H, 2.97. ICP
 40 analysis calcd for Nd: 16.23%. Found: 15.76%. Selected IR data
 (KBr, cm⁻¹): 3456 (mb), 3075 (w), 2836 (w), 1598 (s), 1556 (s), 1516 (m), 1489 (m), 1447 (m), 1420 (s), 1394 (s), 1223 (m), 1155 (m), 1066 (s), 1018 (m), 944 (w), 848 (w), 774 (w), 719 (s), 678 (m), 637 (m), 589 (m), 570 (m), 467 (w), 433 (w), 412 (w).

45

[Mn₈Gd₄(O)₈(hmp)₄(O₂CPh)₁₂(NO₃)₄(PhCO₂H)(C₂H₅OH)] (4)

Yield: 0.084 g, 13%. Elemental analysis (%) calcd for 4: C, 39.78; N, 3.42; H, 3.06. Found: C, 39.83; N, 3.53; H, 3.14. ICP
 45 analysis calcd for Gd: 17.45%. Found: 16.96%. Selected IR data
 (KBr, cm⁻¹): 3443 (mb), 3075 (w), 2843 (w), 2353 (w), 1617 (s), 1556 (s), 1516 (m), 1482 (m), 1455 (m), 1420 (s), 1373 (s), 1312 (s), 1230 (w), 1182 (w), 1148 (w), 1060 (m), 1045 (m), 944 (w), 848 (w), 821 (w), 760 (w), 719 (s), 671 (m), 631 (m), 603 (m), 549 (m), 474 (w), 433 (w).

55

[Mn₈Dy₄(O)₈(hmp)₄(O₂CPh)₁₂(NO₃)₄(PhCO₂H)(C₂H₅OH)] (5)

Yield: 0.079 g, 12%. Elemental analysis (%) calcd for 5: C, 40.00; N, 3.44; H, 2.94. Found: C, 40.10; N, 3.49; H, 2.96. ICP
 50 analysis calcd for Dy: 17.92%. Found: 17.96%. Selected IR data
 (KBr, cm⁻¹): 3443 (mb), 3068 (w), 2843 (w), 1611 (s), 1577 (s),
 60 1523 (m), 1482 (m), 1420 (s), 1380 (s), 1325 (m), 1257 (w), 1230 (w), 1169 (w), 1060 (m), 1018 (m), 855 (w), 814 (w), 774 (w), 719 (s), 678 (s), 623 (m), 603 (m), 562 (m), 467 (w), 427 (w).

Physical measurements

Elemental analyses (C, H and N) were performed on a Vario
 65 ELIII Elemental Analyzer and the content of lanthanide was determined by Inductively Coupled Plasma optical emission

Cite this: DOI: 10.1039/c0xx00000x

www.rsc.org/xxxxxx

ARTICLE TYPE

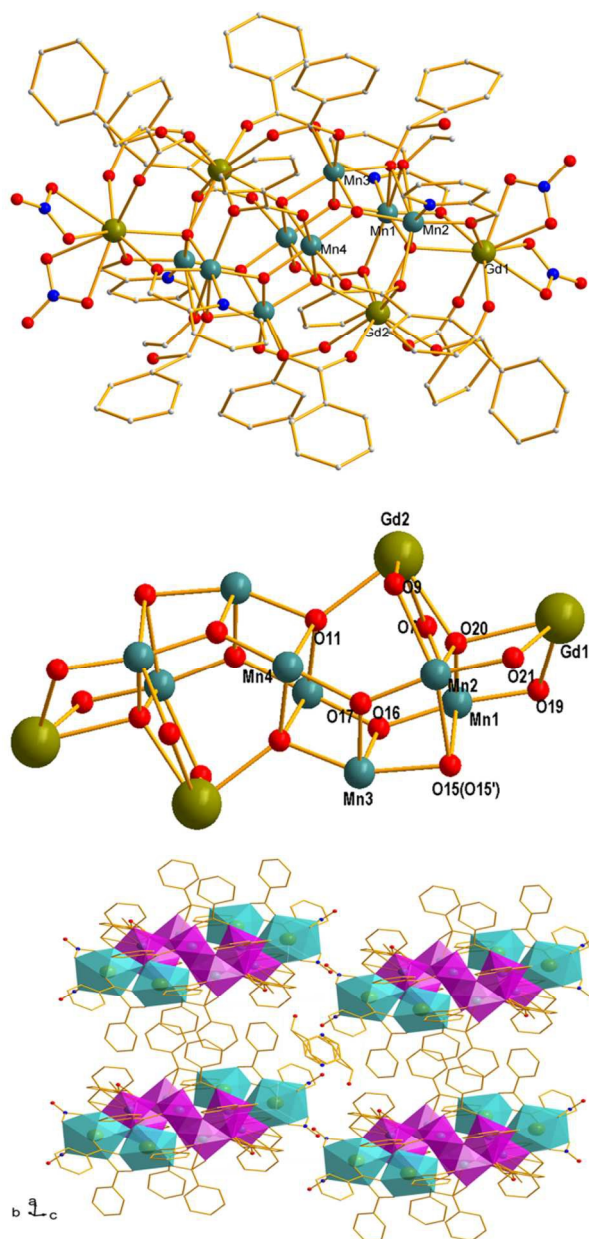


Figure 1. (top) Partially labelled structure of compound **4**, (middle) The core of compound **4**. Color scheme: Gd, green; Mn, teal; O, red; N, blue. (bottom) Polyhedral representation along the $[-1\ 1\ -1]$ direction of the packing of compound **4**. Color scheme: Mn, purple; Gd, green. H atoms have been omitted for clarity.

spectrometer. IR spectra ($400\text{--}4000\text{ cm}^{-1}$) were recorded on a Vertex 70 FT-IR spectrometer in the solid state (KBr pellets). XRPD spectra were measured on a MiniFlexII diffractometer by a Cu-K α rotating anode source with the wavelength of 1.542 Å. (Figure S1) Variable temperature dc susceptibility magnetic

Table 2 Selected bond lengths (Å) and angles (deg) for complex **4**^a

Gd1–O19	2.369(6)	Mn2–O21	1.869(6)
Gd1–O21	2.388(1)	Mn2–O15	2.338(9)
Gd1–O20	2.457(9)	Mn2–O9	2.222(6)
Gd2–O9	2.513(5)	Mn2–O17	1.872(9)
Gd2–O7	2.560(1)	Mn2–O20	1.909(7)
Gd2–O20	2.389(6)	Mn3–O15	2.107(9)
Mn1–O20	1.891(7)	Mn3–O17	1.893(0)
Mn1–O19	1.889(1)	Mn3–O16	1.883(3)
Mn1–O15	2.357(1)	Mn3–O11A	2.004(6)
Mn1–O16	1.874(1)	Mn4–O11A	2.055(9)
Mn4–O11	2.084(5)	Mn4–O17	1.881(1)
Mn4–O16A	1.884(6)		
Gd1–O20–Gd2	112.2(1)	Gd1–O19–Mn1	106.1(8)
Gd1–O21–Mn2	106.8(4)	Mn1–O15–Mn2	84.5(0)
Mn1–O20–Gd2	113.1(5)	Mn1–O16–Mn3	113.4(8)
Mn1–O20–Mn2	112.3(2)	Mn1–O16–Mn4A	133.8(7)
Mn2–O9–Gd2	98.2(4)	Mn2–O15–Mn3	89.9(7)
Mn2–O17–Mn3	113.4(2)	Mn3–O17–Mn4	103.9(0)
Mn3–O11A–Mn4A	93.4(2)	Mn4–O11A–Mn3	94.0(8)
Mn4A–O11–Gd2	122.9(5)	Mn4–O11–Mn4A	93.5(0)

^a Symmetry code: A, $-x+2, -y, -z+1$

data for complexes **1–5** were obtained by a PPMS-9T superconducting magnetometer with a field of 0.1 T and temperature ranging from 2 to 300 K. AC magnetic susceptibilities were collected on a Quantum Design MPMS-XL magnetometer. This magnetometer operates with an oscillating ac field of 3 G in the ac frequencies range 511–2311 Hz.

X-ray crystallography

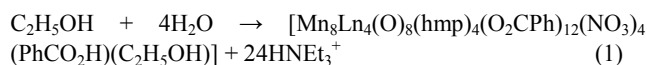
The single crystal data of compounds were collected by a Cu-K α or Mo-K α rotating anode source at 100K, using a Supernova diffractometer with the ω -scan method. Absorption correction was performed with SCALE3 ABSPACK scaling algorithm, using spherical harmonics. All structures were solved with direct methods and full-matrix least-squares refinement were implemented by the SHELXTL-97 program package.²⁰ The non-H atoms were refined anisotropically, while the H atoms were determined with geometrical calculations riding on the respective C atoms. The solvent molecules of complexes were disordered and could not be refined satisfactorily, which were handled with the SQUEEZE option in PLATON.²¹ For compound **4**, the O15/O15' ligand position has a disorder between a PhCO₂H and a C₂H₅OH, and the occupation factors of the PhCO₂H/C₂H₅OH disordered ligands are fixed at 0.5. The crystal data and structure refinement details of complexes are displayed in Table 1.

Results and discussion

Synthesis

Reaction of Mn(NO₃)₂ with hmpH, benzoic acid, NEt₃ and Ln(NO₃)₃·6H₂O (Ln = La; Pr; Nd; Gd; Dy) in MeCN/EtOH (20/5, v/v) afforded a family of [Mn^{III}₈Ln^{III}₄] clusters. The formation of [Mn^{III}₈Ln^{III}₄] clusters is summarized in eq 1:

$$8\text{Mn}^{2+} + 4\text{Ln}^{3+} + 4\text{hmpH} + 24\text{NEt}_3 + 4\text{NO}_3^- + 2\text{O}_2 + 13\text{PhCO}_2\text{H} +$$



The NEt_3 is assumed to be the proton acceptor, but also promoted the oxidation reaction of Mn^{II} to $\text{Mn}^{\text{III}}/\text{Mn}^{\text{IV}}$ with atmospheric O_2 by providing alkaline conditions. A variety of conditions have been explored, such as different reagent ratios and solvents. While using only MeCN as the solvent led to another family of compounds in low yield, the study of which is in progress. When reagent ratios were changed, it only affected the yield and purity of **1–5**, with the $[\text{Mn}^{\text{III}}_8\text{Ln}^{\text{III}}_4]$ as the only crystallized products.

Description of the crystal structures

Compounds **1–5** are isostructural, therefore the structure of compound **4** will be described in detail as representative of this series. The partially labeled structure and core of complex **4** is shown in Figure 1. Selected interatomic distances and angles are presented in Table 2 (For others, selected interatomic distances and angles are presented in Table S3 to S6). Compound **4** crystallizes in the triclinic space group $P-1$, and possesses a spindle-shaped core, $[\text{Mn}^{\text{III}}_8\text{Gd}^{\text{III}}_4(\mu_4\text{-O})_4(\mu_3\text{-O})_4(\mu_3\text{-OR})_2(\mu_2\text{-OR})_8]^{10+}$ core (Figure 1). The core comprises six face-sharing defected cubane units, two $\text{Mn}_3(\mu_4\text{-O})_2(\mu_3\text{-O})_2$, two $\text{Mn}_3(\mu_4\text{-O})(\mu_3\text{-O})_2(\mu_3\text{-OR})$ and two terminal $\text{Mn}_2\text{Gd}(\mu_4\text{-O})(\mu_3\text{-OR})(\mu_2\text{-OR})_2$, which connect to two square-pyramidal units, $\text{Gd}(\mu_4\text{-O})(\mu_3\text{-O})(\mu_2\text{-OR})_2$, via two $\mu_4\text{-O}$, two $\mu_3\text{-O}$ and four $\mu_2\text{-O}$ atoms. The two benzoic acid groups each provide the $\mu_3\text{-OR}$ ($\text{O}15/\text{O}15'$) atoms bridging three Mn (Mn1, Mn2, Mn3) atoms in the $\eta^3:\mu_3$ mode. The four MnGd pairs are respectively coordinated with a carboxylate group in their $\eta^1:\eta^2:\mu_3$ mode, while another four MnGd units are each bridged by the alkoxide O atom of an $\eta^1:\eta^2:\mu$ hmp⁻ group. The peripheral ligation is completed by eight deprotonated $\eta^1:\eta^1:\mu_2$ carboxylate ligands and four chelating $\eta^1:\eta^1:\mu_1$ NO_3^- ligands.

The oxidation states of Mn atoms and the protonation level of O atoms were established by the metric parameters and charge balance consideration, which confirmed by bond valence sum (BVS)^{22a} calculations (Tables S1 and S2, respectively). All Mn^{III} ions are six coordinate possessing distorted octahedral geometries. Mn1, Mn2 and their symmetry equivalent ions exhibit distinct Jahn-Teller (JT) axial elongations along $\text{O}7\text{--Mn}1\text{--O}15$, $\text{O}9\text{--Mn}2\text{--O}15$ axes and their symmetry-related axes, with the elongated Mn–O bonds containing Mn1–O7 (2.197 Å), Mn1–O15 (2.358 Å), Mn2–O9 (2.223 Å) and Mn2–O15 (2.345 Å) evidently longer than the others (1.871–2.034 Å). The Gd1 is coordinated by nine oxygen atoms with a distorted triaugmented triangular prism geometry: one is $\mu_4\text{-O}$ that bridges Mn1, Mn2 and Gd2, another four are from two benzoic acid ligands and two $\eta^1:\eta^2:\mu$ hmp⁻ groups, and the other four are from two NO_3^- ligands. Gd2 is coordinated by eight oxygen atoms: Six are from benzoic acid ligands, including two $\mu_2\text{-OR}$ that bridged Gd2 to Mn1 and Mn2 respectively, and the rest are two $\mu_4\text{-O}$ coordinated Gd2 with other metal atoms. Its coordination polyhedron may be described as a distorted square antiprism. There are no close intermolecular interactions between the molecules, the nearest neighbour metal-metal distance between different molecules is the distance of Gd–Gd (8.059 Å), thus the magnetic behaviour of the complexes is considered to be of molecular origin.^{22b}

To the best of our knowledge, so far, only a small amount of dodecanuclear Mn/Ln aggregates have been reported, including

Table 3 Summary of direct current magnetic data for compounds **1–5**

Compound	Expected $\chi_{\text{M}}T$ at 300 K ^a	Experimental $\chi_{\text{M}}T$ at 300 K ^a	Experimental $\chi_{\text{M}}T$ at 2 K ^a	Curie constant C^a	Weiss constant θ^b
1	24.01	23.65	40.09	23.27	4.95
2	30.41	29.94	45.08	29.17	3.56
3	30.57	29.56	30.34	28.64	7.43
4	55.53	55.27	53.11	54.37	5.11
5	80.69	78.04	64.10	77.40	-0.05

Units: ^a $\text{cm}^3 \text{K mol}^{-1}$. ^b K.

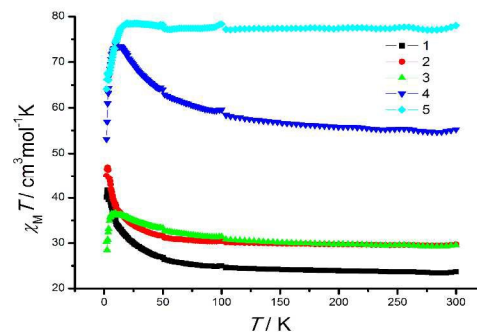


Figure 2 Plots of $\chi_{\text{M}}T$ vs. T for compounds **1–5**.

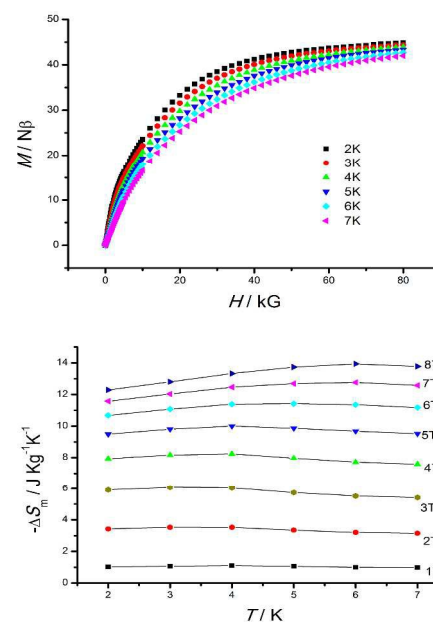


Figure 3 (top) Field-dependent magnetization at indicated temperature (2–7 K) for complex **4**. (bottom) temperature dependence of magnetic entropy change of complex **4**.

the distorted hexagonal bipyramid $[\text{Mn}^{\text{III}}_{10}\text{Ln}^{\text{III}}_2]$,^{23a} the bell-shaped $[\text{Mn}^{\text{III}}_9\text{Mn}^{\text{II}}_2\text{Ln}^{\text{III}}]$,^{23b} $[\text{Mn}^{\text{III}}_4\text{Mn}^{\text{IV}}_2\text{Dy}^{\text{III}}_6]$ ^{23c} comprising nearly planar hexagonal ring capped by a trimer on either end, the truncated-ball shaped $[\text{Mn}^{\text{II}}_6\text{Dy}^{\text{III}}_6]$,^{23d} the butterfly-shaped $[\text{Mn}^{\text{III}}_6\text{Ln}^{\text{III}}_6]$,^{23f} and two offset stacked symmetry-related 14-metallacrown (MC)-5 ring of $[\text{Mn}^{\text{III}}_8\text{Ln}^{\text{III}}_4]$ ^{23e} units. Obviously, the structures of complexes **1–5** are completely different from these compounds above, which represent a new topology.

Magnetic properties

The solid-state, variable-temperature dc magnetic susceptibility

data of compounds **1–5** were measured in the 2–300 K temperature range with an applied field of 0.1 T. Plots of $\chi_M T$ vs. T for compounds **1–5** are depicted in Figure 2. At room temperature, the $\chi_M T$ values of compounds **1–5** are in relatively good agreement with the expected value for the uncoupled $\text{Mn}^{\text{III}}_8\text{Ln}^{\text{III}}_4$ core (Table 3). For compounds **1** and **2**, the $\chi_M T$ vs. T plots show similar trends, in which the $\chi_M T$ increase monotonically to maximum value of $41.68 \text{ cm}^3 \text{ K mol}^{-1}$ and $46.90 \text{ cm}^3 \text{ K mol}^{-1}$ respectively at 3 K upon cooling and then slightly decrease to $40.09 \text{ cm}^3 \text{ K mol}^{-1}$ and $45.08 \text{ cm}^3 \text{ K mol}^{-1}$ at 2 K. For compounds **3** and **4**, the $\chi_M T$ increase with decreasing temperature from $29.56 \text{ cm}^3 \text{ K mol}^{-1}$ and $55.26 \text{ cm}^3 \text{ K mol}^{-1}$ at 300 K to maximum of $36.42 \text{ cm}^3 \text{ K mol}^{-1}$ at 8 K and $73.93 \text{ cm}^3 \text{ K mol}^{-1}$ at 10 K, and then abruptly decrease to $28.48 \text{ cm}^3 \text{ K mol}^{-1}$ and $53.11 \text{ cm}^3 \text{ K mol}^{-1}$ at 2 K, respectively. The low-temperature decrease of $\chi_M T$ for compounds **1–4** as expected due to the magnetic anisotropy, and/or weak intermolecular interactions.²⁴ The overall shape of $\chi_M T$ vs. T curves and the positive Weiss constants for compounds **1–4** indicate dominate ferromagnetic interactions within these compounds, which is different from the other three clusters with the use of hmpH which exhibit antiferromagnetic interactions.¹⁹ For compound **5**, the $\chi_M T$ value stays essentially constant with decreasing temperature until approximately 20 K, and then rapidly decreases down to $64.10 \text{ cm}^3 \text{ K mol}^{-1}$ at 2 K. The decrease of the $\chi_M T$ value for compound **5** is probably arises from the thermal depopulation of the Stark sublevels, which arises from the crystal field splitting of the $^6\text{H}_{15/2}$ state for Dy^{III} ion.²⁶ As La^{III} ion is diamagnetic, the magnetic property of ferromagnetic for **1** is only attributed to the exchange interactions between Mn–Mn. We can subtract the plot 1 from 4 to investigate the interactions between Gd–Gd and Gd–Mn in complex **4**, the $\chi_M T$ product increase with decreasing temperature (Figure S2) suggesting the interactions between Gd–Gd and/or Gd–Mn are ferromagnetic.

Ferromagnetic interactions between Gd–Gd ions have been reported in recent years. In these examples the separations of Gd–Gd are in the range of 3.72–4.93 Å, and the angles at the bridging oxygen atoms in the range of 96–140°. In compound **4**, the Gd–Gd separation is 4.024 Å and the Gd–O–Gd angle is 112°, the structural parameters indicate that the $[\text{Gd}_2]_2$ units may be ferromagnetic. While in these systems, magnetic coupling interactions of the compounds **2**, **3** and **5** are difficult to investigate because of the complicated intrinsic magnetic properties of the Pr^{III} , Nd^{III} and Dy^{III} ions.^{28f}

The concept that negligible anisotropy and ferromagnetic exchange have advantage of constructing large MCE²⁵ urged us to explore the MCE of complex **4**. The M versus H data were collected under 2–7 K at 1–8 T (Figure 3). As the MCE can be described as the Maxwell equation $-\Delta S_m = \int [\partial M(T, H) / \partial T]_{\text{H}} dH$, the maximum value of $-\Delta S_m$ is $13.94 \text{ J Kg}^{-1} \text{ K}^{-1}$ at 6 K for $\Delta H = 8 \text{ T}$ (Figure 3). The value is larger than the theoretical maximum entropy of $8.85 \text{ J Kg}^{-1} \text{ K}^{-1}$ calculated according to the equation $R \ln(2S + 1)$ for an isolated $S = 22$ ($S = 8 + (4 * 7/2)$) spin ground state (Table 4). This indicates that the presence of low-lying excited states for compound **4** have a positive influence on the MCE.³⁰

For compound **1**, the magnetization data were collected in the dc magnetic field range 0.1–5 T at 2.0–15.0 K to investigate the

Table 4 The entropy change for compound **4**.

	Expected $-\Delta S_m$	Experimental $-\Delta S_m$
$-\Delta S_m^a$	8.85	13.94
$-\Delta S_m^b$	31.64	49.83

Units: ^a $\text{J Kg}^{-1} \text{ K}^{-1}$, ^b $\text{J mol}^{-1} \text{ K}^{-1}$.

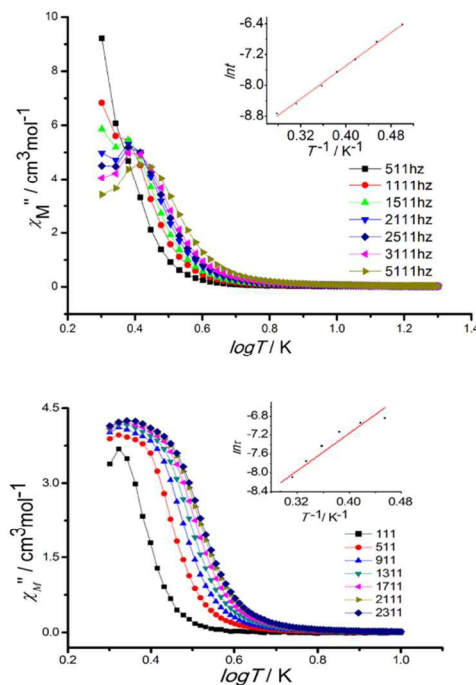


Figure 5 (top) out-of-phase χ''_M ac susceptibility signals for complex **5** in a 3.0 G field oscillating with a zero dc field, (bottom) out-of-phase χ''_M ac susceptibility signals for complex **1** in a 3.0 G field oscillating with an applied dc field of 500 Oe. The $\ln \tau$ vs. $1/T$ plots (inset) and the value of τ_0 can be extracted from the slope.

anisotropy and the ground state of the compound, as shown in Figure S3. The data of complex **1** were fitted using the program ANISOFIT 2.0,²⁴ assuming only the spin ground state of the molecule is populated and the corresponding spin Hamiltonian employed to fit is $\hat{H} = D\hat{S}_z^2 + E(\hat{S}_x^2 + \hat{S}_y^2) + g_{\text{iso}}\mu_B\hat{S}\cdot B$. The best fits are obtained, with the parameters $S = 8$, $g = 2.05$ and $D = -0.1693 \text{ cm}^{-1}$, at low fields (0.1 T, 0.5 T, 1 T) so as to avoid problems from low-lying excited states. The value of g is slightly larger than the value of most Mn/Ln complexes. The reason for this may be that the electrons are still populated in the low-lying excited states at low fields.³³ Alternative fit of $S = 6$ or 10 gave unreasonable value of g and was rejected. Furthermore, the M value for compound **1** under 2 K at 8 T is $15.71 \text{ N}\mu_B$ (Figure S5), it is approximate to the calculated value $16 \text{ N}\mu_B$ (gS). While, it may exist weak and competing antiferromagnetic and ferromagnetic exchange for compound **1** that leads to such an intermediate ground spin state. The isothermal magnetization curves (M vs. H/T) for compounds **1**, **2**, **4** and **5** (Figure S4) are non-coincident, displaying the presence of magnetic anisotropy of Ln^{III} or low-lying excited states.²⁷ The magnetization of these compounds increases slowly with increasing applied field without saturation even at 8 T (Figure S5 and S6), which further confirmed the presence of these effects.

The ac susceptibility measurements were performed on complexes **1–5** in the temperature range of 2.0 K to 5.0 K with a

3.0 G ac field oscillating in the scope of 511 Hz–5111 Hz and a zero-applied dc field. Compound **5** showed a frequency-dependent decrease in $\chi_M T$ indicating slow magnetic relaxation, and the out-of-phase χ_M'' signals displayed concomitant appearance thus indicating probably SMM behaviour. The other compounds appear to reveal a small out of phase component in the ac data at low temperature but there is no clear maximum in χ_M'' diagnostic of SMM like behaviour (Figure S7 to S10). It should be noted that the maximum of the peak appeared for compound **1** with an applied 500 Oe dc field. As La^{III} ion is diamagnetic, it is concluded that slow relaxation could arise from the Mn ions solely. The two complexes displayed out-of-phase χ_M'' peak maximum (Figure 5). We fitted the cusp of out-of-phase susceptibility data for complexes **1** and **5** with Arrhenius law, which generalized the correlations of the relaxation time τ and anisotropy barrier U_{eff} as the equation: $\tau = \tau_0 \exp(U_{\text{eff}}/k_B T)$. The results show that there is a linear relationship between $\ln \tau$ versus $1/T$ (Figure 5 inset), giving $\tau_0 = 1.48 \times 10^{-5}/7.68 \times 10^{-6}$ s and $U_{\text{eff}} = 6.88/7.44$ K.

Conclusions

In summary, reactions of Mn(NO₃)₂ and Ln(NO₃)₃·6H₂O with hmpH and benzoic acid as co-ligands have yielded new examples of 3d/4f dinuclear clusters. The flexible benzoic acid and the bidentate ligand hmpH have been used as co-ligands for the first time to synthesize Mn/Ln clusters, and the Mn₈Ln₄ cluster has the highest nuclearity among Mn/Ln clusters used hmpH so far. These complexes are new additions to the very small family of dinuclear Mn/Ln clusters, and each compound possesses a spindle-shaped novel core. Solid-state dc magnetic susceptibility analyses suggest that the ferromagnetic interactions dominated within complex **1-4**. Compound **4** displays an MCE with 13.94 J Kg⁻¹ K⁻¹ of the entropy change at 6 K for $\Delta H = 8$ T. Ac magnetic susceptibility investigations showed a frequency-dependent decrease in $\chi_M T$ and out-of-phase χ_M'' peak maximum, indicating slow magnetic relaxation and potential SMM behaviour for complexes **1** and **5**.³⁴

Acknowledgement

This work was supported by the National Natural Science Foundation of China (Nos. 21173219, 21303201 and 21203195).

Notes and references

a State Key Laboratory of Structural Chemistry, Fujian Institute of Research on the Structure of Matter, The Chinese Academy of Sciences, Fuzhou, Fujian 350002, China. Fax: +86 591 83792395; E-mail: ccn@fjirsm.ac.cn

b University of Chinese Academy of Sciences, Beijing 100039, China.

† Electronic Supplementary Information (ESI) available: [X-ray crystallographic data for complexes **1–5** in CIF format. CCDC 1045933, 1045934, 1045935, 1045936 and 1045937]. See DOI: 10.1039/b000000x/1(a) R. Sessoli, T. Sai, H. L. A. R. Schake, S. Wang, J. B. Vincent, K. Folting, D. Gatteschi, G. Christou and D. N. Hendrickson, *J. Am. Chem. Soc.*, 1993, 115, 1804; (b) D. Gatteschi and R. Sessoli, *Angew. Chem., Int. Ed.*, 2003, 42, 268; (c) G. Aromil and E. K. Brechin, *Struct. Bonding (Berlin)* 2006, 122, 1; (d) D. P. Goldberg, A. Caneschi, C. D. Delfs, R. Sessoli and S. J. Lippard, *J. Am. Chem. Soc.*, 1995, 117, 5789.

2(a) D. Ruiz, Z. Sun, B. Albel, K. Folting, J. Ribas, G. Christou and D. N. Hendrickson, *Angew. Chem. Int. Ed.*, 1998, 37, 300; (b) A. M.

- Ako, I. J. Hewitt, V. Mereacre, R. Clerac, W. Wernsdorfer, C. E. Anson and A. K. Powell, *Angew. Chem. Int. Ed.*, 2006, 45, 4926; (c) M. Murugesu, *Nat. Chem.*, 2012, 4, 347; (d) M. Nakano and H. Oshio, *Chem. Soc. Rev.*, 2011, 40, 3239; (e) C. Boskovic, W. Wernsdorfer, K. Folting, J. C. Huffman, D. N. Hendrickson and G. Christou, *Inorg. Chem.*, 2002, 41, 5107; (f) M. Wang, D. Q. Yuan, C. B. Ma, M. J. Yuan, M. Q. Hu, N. Li, H. Chen, C. N. Chen and Q. T. Liu, *Dalton Trans.*, 2010, 39, 7276.
- 3(a) E. K. Brechin, C. Boskovic, W. Wernsdorfer, J. Yoo, A. Yamaguchi, E. C. Sanudo, T. R. Concolino, A. L. Rheingold, H. Ishimoto, D. N. Hendrickson and G. Christou, *J. Am. Chem. Soc.*, 2002, 124, 9710; (b) D. Ruiz, Z. Sun, B. Albel, K. Folting, J. Ribas, G. Christou and D. N. Hendrickson, *Angew. Chem. Int. Ed.*, 1998, 37, 300; (c) W. Wernsdorfer, S. Bhaduri, C. Boskovic, G. Christou and D. N. Hendrickson, *Phys. Rev. B*, 2002, 65, 180403(1); (d) W. Wernsdorfer, M. Soler, G. Christou and D. N. Hendrickson, *J. Appl. Phys.*, 2002, 91, 7164; (e) C. Lampropoulos, M. Murugesu, A. G. Harter, W. Wernsdorfer, S. Hill, N. S. Dalal, A. P. Reyes, P. L. Kuhns, K. A. Abboud and G. Christou, *Inorg. Chem.*, 2013, 52, 258.
- 4(a) R. Bagai and G. Christou, *Chem. Soc. Rev.*, 2009, 38, 1011; (b) L. Bogani and W. Wernsdorfer, *Nat. Mater.*, 2008, 7, 179; (c) G. Christou, D. Gatteschi, D. N. Hendrickson and R. Sessoli, *MRS Bull.*, 2000, 25, 66; (d) M. N. Leuenberger and D. Loss, *Nature*, 2001, 410, 789; (e) A. K. Powell, *Nat. Chem.*, 2010, 2, 351.
- 5 S. Osa, T. Kido, N. Matsumoto, N. Re, A. Pochaba and J. Mrozinski, *J. Am. Chem. Soc.*, 2004, 126, 420.
- 6(a) L. F. Zou, L. Zhao, Y. N. Yu, Y. Guo, J. K. Tang and Y. H. Li, *Chem. Commun.*, 2011, 47, 8659; (b) H. L. C. Feltham, R. Clerac, A. K. Powell and S. Brooker, *Inorg. Chem.*, 2011, 50, 4232; (c) S. K. Langley, L. Ungur, N. F. Chilton, B. Moubaraki, L. F. Chibotaru and K. S. Murray, *Chem.-Eur. J.*, 2011, 17, 9209; (d) V. Chandrasekhar, B. M. Pandian, R. Boomishankar, A. Steiner, J. J. Vifal, A. Hourri and R. Clerac, *Inorg. Chem.*, 2008, 47, 4918; (e) Y. F. Zeng, G. C. Xu, X. Hu, Z. Chen, X. H. Bu, S. Gao and E. C. Sanudo, *Inorg. Chem.*, 2010, 49, 9734; (f) M. Zaleski, E. C. Depperman, J. W. Kampf, M. L. Kirk and V. L. Pecoraro, *Angew. Chem., Int. Ed.*, 2004, 43, 3912.
- 7 A. Mishra, W. Wernsdorfer, S. Parsons, G. Christou and E. K. Brechin, *Chem. Commun.*, 2005, 2086.
- 8 J. Y. Liu, C. B. Ma, H. Chen, M. Q. Hu, H. M. Wen, H. H. Cui, X. W. Song and C. N. Chen, *Dalton Trans.*, 2013, 42, 11, 3787.
- 9(a) A. Saha, M. Thompson, K. A. Abboud, W. Wernsdorfer and G. Christou, *Inorg. Chem.*, 2011, 50, 10476; (b) P. S. Koroteev, Z. V. Dobrokhotova, A. B. Ilyukhin and V. M. Novotortsev, *Polyhedron*, 2013, 65, 110; (c) H. S. Ke, L. Zhao, Y. Guo and J. K. Tang, *Dalton Trans.*, 2012, 41, 2314.
- 10(a) V. Mereacre, A. M. Ako, R. Clerac, W. Wernsdorfer, I. J. Hewitt, C. E. Anson and A. K. Powell, *Chem. Eur. J.*, 2008, 14, 3577; (b) T. C. Stamatatos, S. J. Teat, W. Wernsdorfer and G. Christou, *Angew. Chem., Int. Ed.*, 2009, 48, 521; (c) A. M. Ako, V. Mereacre, R. Clerac, W. Wernsdorfer, I. J. Hewitt, C. E. Anson and A. K. Powell, *Chem. Commun.*, 2009, 544.
- 11 M. Evangelisti, F. Luis, L. J. de Jongh and M. Affronte, *J. Mater. Chem.*, 2006, 16, 2534.
- 12(a) P. A. Debye, *Phys.*, 1926, 81, 1154. (b) W. F. Giaque, *J. Am. Chem. Soc.*, 1927, 49, 1864; (c) M. Evangelisti and E. K. Brechin, *Dalton Trans.*, 2010, 39, 4672; (d) C. T. Tian, Z. J. Lin and S. W. Du, *Cryst. Growth Des.*, 2013, 13, 3746; (e) Y. C. Chen, F. S. Guo, J. L. Liu, J. D. Leng, P. Vrebel, M. Orendac, J. Prokleska, V. Sechovsky and M. L. Tong, *Chem. Eur. J.*, 2014, 20, 3029.
- 13(a) S. K. Langley, N. F. Chilton, B. Moubaraki, T. Hooper, E. K. Brechin, M. Evangelisti and K. S. Murray, *Chem. Sci.*, 2011, 2, 1166; (b) M. Evangelisti, O. Roubeau, E. Palacios, A. Camn, T. N. Hooper, E. K. Brechin and J. J. Alonso, *Angew. Chem. Int. Ed.*, 2011, 50, 6606; (c) F. S. Guo, Y. C. Chen, J. L. Liu, J. D. Leng, Z. S. Meng, P. Vrebel, M. Orendac and M. L. Tong, *Chem. Commun.*, 2012, 48, 12219.
- 14 T. C. Stamatatos, K. M. Poole, K. A. Abboud, W. Wernsdorfer, T. A. O'Brien and G. Christou, *Inorg. Chem.*, 2008, 47, 5006.
- 15 N. C. Harden, M. A. Bolcar, W. Wernsdorfer, K. A. Abboud, W. E. Streib and G. Christou, *Inorg. Chem.*, 2003, 42, 7067.

- 16 E.C. Sanudo, W. Wernsdorfer, K.A. Abboud and G. Christou, *Inorg. Chem.*, 2004, 43, 4137.
- 17 C. Boskovic, E. K. Brechin, W. E. Streib, K. Folting, J. C. Bollinger, D. N. Hendrickson and G. Christou, *J. Am. Chem. Soc.*, 2002, 124, 3725.
- 18 E. C. Sanudo, E. K. Brechin, C. Boskovic, W. Wernsdorfer, J. Yoo, A. Yamaguchi, T. R. Concolino, K. A. Abboud, A. L. Rheingold, H. Ishimoto, D. N. Hendrickson and G. Christou, *Polyhedron*, 2003, 22, 2267.
- 19(a) C. Papatriantafyllopoulou, W. Wernsdorfer, K. A. Abboud and G. Christou, *Inorg. Chem.*, 2011, 50, 421; (b) J. Feuersenger, D. Prodius, V. Mereacre, R. Clérac, C. E. Anson and A. K. Powell, *Inorganic Chemistry Communications*, 2011, 14, 1851; (c) C. Papatriantafyllopoulou, K. A. Abboud and G. Christou, *Polyhedron*, 2013, 52, 196.
- 20 G. M. Sheldrick, SHELXTL, 5.0, Siemens Analytical X-ray Instruments Inc., Madison, Wisconsin, USA, 1997.
- 21 P. Van der sluis and A. L. Spek, *Acta Crystallogr., Sect. A: Found. Crystallogr.*, 1990, 46, 194.
- 22 (a) I. D. Brown and D. Altermatt, *Acta Crystallogr., Sect. B: Struct. Sci.*, 1985, 41, 244; (b) H. Chen, C. B. Ma, M. Q. Hu, H. M. Wen, H. H. Cui, J. Y. Liu, X. W. Song and C. N. Chen, *Dalton Trans.*, 2013, 42, 4908.
- 23(a) V. Mereacre, D. Prodius, A. M. Ako, N. Kaur, J. Lipkowski, Ch. Simmons, N. Dalal, I. Geru, C. E. Anson, A. K. Powell and C. Turta, *Polyhedron*, 2008, 27, 2459; (b) V. Mereacre, Y. H. Lan, W. Wernsdorfer, C. E. Anson and A. K. Powell, *C. R. Chimie*, 15, 2012, 639; (c) M. Z. Curtis, E. C. Depperman, J. W. Kampf, M. L. Kirk, and V. L. Pecoraro, *Angew. Chem. Int. Ed.*, 2004, 43, 3912; (d) Y. Z. Zheng, E. M. Pineda, M. Helliwell and R. E. P. Winpenny, *Chem. Eur. J.*, 2012, 18, 4161; (e) F. Cao, S. N. Wang, D. C. Li, S. Y. Zeng, M. J. Niu, Y. Song and J. M. Dou, *Inorg. Chem.*, 2013, 52, 10747; (f) T. G. Tziotzi, D. I. Tzimopoulos, T. Lis, R. Inglis and C. J. Milios, *Dalton Trans.*, 2015, 44, 11696.
- 24 M. Hołyn, D. Premuz'ic', I. Jeon, W. Wernsdorfer, R. Clrac and S. Dehnen, *Chem. Eur. J.*, 2011, 17, 9605.
- 25(a) J. P. Zhao, R. Zhao, Q. Yang, B. W. Hu, F.-C. Liu and X. H. Bu, *Dalton Trans.*, 2013, 42, 14509; (b) F. S. Guo, Y. C. Chen, J. L. Liu, J. D. Leng, Z. S. Meng, P. Vrbel, M. Orendac and M. L. Tong, *Chem. Commun.*, 2012, 48, 12219; (c) Y. C. Chen, F. S. Guo, J. L. Liu, J. D. Leng, P. Vrbel, M. Orendac, J. Prokleska, V. Sechovsky and M. L. Tong, *Chem. Eur. J.*, 2014, 20, 3029; (d) Y. Z. Zheng, E. M. Pineda, M. Helliwell and R. E. P. Winpenny, *Chem. Eur. J.*, 2012, 18, 4161; (e) S. K. Langley, N. F. Chilton, B. Moubaraki, T. Hooper, E. K. Brechin, M. Evangelisti and K. S. Murray, *Chem. Sci.*, 2011, 2, 1166; (f) G. Lorusso, M. A. Palacios, G. S. Nichol, E. K. Brechin, O. Roubeau and M. Evangelisti, *Chem. Commun.*, 2012, 48, 7592.
- 28 G. Karotsis, S. Kennedy, S. J. Teat, C. M. Beavers, D. A. Fowler, J. J. Morales, M. Evangelisti, S. J. Dalgarno and E. K. Brechin, *J. Am. Chem. Soc.*, 2010, 132, 12983.
- 29(a) S. Nayak, M. Evangelisti, A. K. Powell and J. Reedijk, *Chem. Eur. J.*, 2010, 16, 12865; (b) M. Manoli, R. D. L. Johnstone, S. Parsons, M. Murrie, M. Affronte, M. Evangelisti and E. K. Brechin, *Angew. Chem. Int. Ed.*, 2007, 119, 4456; (c) M. Manoli, A. Collins, S. Parsons, A. Candini, M. Evangelisti and E. K. Brechin, *J. Am. Chem. Soc.*, 2008, 130, 11129.
- 30 J. P. Sutter and M. L. Kahn, *Lanthanide Ions in Molecular Exchange Coupled Systems. In Magnetism: Molecules to Materials V*, Wiley-VCH Verlag GmbH & Co. KGaA: 2005, pp 161.
- 31 J. L. Liu, W.Q. Lin, Y. C. Chen, C. C. Silvia, A. Daniel, E. Ruiz, J. D. Leng and M. L. Tong, *Chem. Eur. J.*, 2013, 19, 17567.
- 32 (a) Y. C. Chen, F. S. Guo, J. L. Liu, J. D. Leng, P. Vrbel, M. Orendac, J. Prokleska, V. Sechovsky and M. L. Tong, *Chem. Eur. J.*, 2014, 20, 3029; (b) G. Karotsis, S. Kennedy, S. J. Teat, C. M. Beavers, D. A. Fowler, J. J. Morales, M. Evangelisti, S. J. Dalgarno and E. K. Brechin, *J. Am. Chem. Soc.*, 2010, 132, 12983.
- 33 (a) C. papatriantafyllopoulou, KA Abboud, G Christou, *Polyhedron*, 2013, 52, 196; (b) H. S. Wang, X. J. Song, H. B. Zhou, Y. Chen, Y. L. Xu and Y. Song, *Polyhedron*, 2011, 30, 3206.
- 34 (a) B. Monteiro, J. T. Coutinho, C. C. L. Pereira, L. C. J. Pereira, J. Marçalo, M. Almeida, J. J. Baldoví, E. Coronado and A. Gaita-Ariño, *Inorg. Chem.*, 2015, 54, 1949; (b) J. J. Baldoví, J. M. Clemente-Juan, E. Coronado, Y. Duan, A. Gaita-Ariño and C. Giménez-Saiz, *Inorg. Chem.*, 2014, 53, 9976.